Satellite Drag Perturbations in an Oblate Diurnal Atmosphere

F. A. Santora*
General Electric Company, Valley Forge, Pa.

Analytic expressions are derived that describe decay rates in period and eccentricity, and rotation in perigee argument for orbits of small eccentricity ($e<0.2$). The equations include both the oblate earth figure and diurnal density effects and represent an extension to available theory which treat these effects separately. Ancillary equations are also developed to account for gravitational perigee perturbations which can cause errors in decay rates of 15%, and for proper scale height selection which can be another error source of 5%. Comparison with numerical methods show inherent decay rate accuracies to within 2% and that computational times are reduced by two orders of magnitude for prediction of orbit decay histories. Results also indicate that day-to-night density variation has little effect on eccentric orbits greater than 0.1.

Introduction

SINCE the atmosphere is dynamic and varies considerably during the lifetime of a satellite, accurate decay histories are not easily or rapidly obtained. However, if realistic perturbation expressions are available and atmosphere parameters are updated as required, both drag and gravitational perturbations can be quickly estimated and summed to give reasonably accurate decay histories without numerical integration. Previously, the effect of atmosphere drag perturbations on artificial satellite orbits of small eccentricity ($e<0.2$) in an oblate atmosphere was studied by Cook, King-Hele, Walker,[1,2] and others. In their theory, equations for predicting decay rates in orbit period, eccentricity and other parameters were derived. In a separate development, Cook, King-Hele[3] extended the theory to include the day-to-night density variation (atmosphere bulge) by assuming a sinusoidal density variation with geocentric angular distance from the maximum density point. However, the extended theory is limited to a spherical earth figure. This paper unifies the separate theories and provides a single set of analytic expressions having a greater inherent accuracy for predicting decay rates especially for orbits of small eccentricity ($e<0.2$).

Two major error sources in predicting decay rates are the gravitational perturbation of perigee radius, r_p, up to ± 5 naut mile, (± 9 km), and of the perigee argument ω, of $\pm 5\frac{1}{2}°$. Another potential error source involves the proper selection of density scale height, H. Simple formulas are presented for accurate prediction of perigee conditions and suitable scale height selection during the decay process. For consistency with Cook, King-Hele's work, their nomenclature and symbology are retained wherever possible.

Decay Rate Equations

The approach taken to derive the decay rate equations is identical to that originally used by Cook, King-Hele and Walker,[2] except that the sinusoidal variation of density on a constant altitude surface[3] is factored into the oblate atmosphere theory as a variable quantity rather than a constant density value. Figure 1 illustrates the geometry by showing an exaggerated oblate earth figure with a diurnal atmosphere.

Presented as Paper 74-839 at the AIAA Mechanics and Control of Flight Conference, Anaheim California, August 5-9, 1974; submitted September 6, 1974; revision received February 20, 1975.

Index category: Earth-Orbital Trajectories.

*Systems Engineer. Member AIAA.

For purposes of illustration, a polar orbit is shown whose perigee is displaced an angular distance, ϕ, from the bulge center. A constant altitude surface is defined by the satellite altitude, h_p, at the time of perigee passage. The maximum density point on this constant altitude surface is ρ_{max}, and is located[3] at the sub-bulge point. Conversely, the minimum density point, ρ_{min}, is diametrically opposite ρ_{max}. The geocentric radius of the constant altitude surface is denoted by σ, and is taken from Cook King-Hele, Walker[2];

$$\sigma = r_p[1-\epsilon \sin^2 i \sin^2(\omega+\theta)] \cdot [1-\epsilon \sin^2 i \sin^2 \omega]^{-1} \quad (1)$$

which can be expanded to,

$$\sigma = r_p[1-1/2\,\epsilon \sin^2 i \cos 2\omega + 1/2\epsilon \sin^2 i \cos 2(\omega+\theta)] \quad (2)$$

Where ϵ is the earth's flattening factor, i is the orbit inclination, and r_p is the perigee radius. The perigee argument and true anomaly of the satellite are denoted by ω and θ respectively. Density ρ at the satellite radius r can be expressed in terms of σ, the average density ρ_o, a density amplitude factor F, the angular distance ϕ from ρ_{max}, and the inverse of the density scale height $\beta(\beta=1/H)$.

$$\rho = \rho_o(1+F\cos\phi)\exp[-\beta(r-\sigma)] \quad (3)$$

Equation (3) includes the day-to-night density variation in an oblate atmosphere. In amplified form, noting that, $r-r_p=ae$

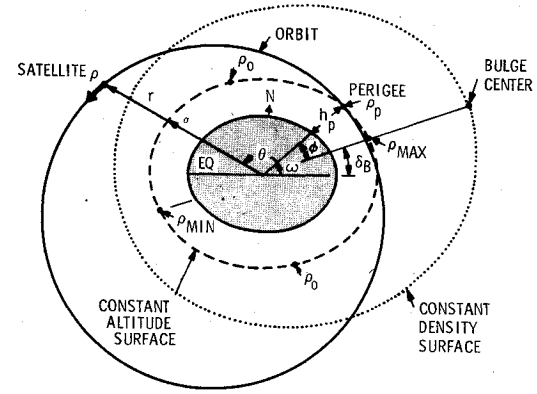

Fig. 1 Geometry description.

$(1-\cos E)$, Eq. (3) becomes

$$\rho=\rho_0(1+FA\cos\theta+FB\sin\theta)$$
$$\cdot\exp[-\beta(1-\cos E)ae-c\cos 2\omega+c\cos 2(\omega+\theta)] \quad (4)$$

Where ρ_0, F, A, B and c have been previously defined[3] but are repeated here for completeness. In Eq. (4) a is the semimajor axis, and E is the eccentric anomaly.

$$\rho_0=1/2(\rho_{\max}+\rho_{\min}) \quad (5)$$

$$F=(\rho_{\max}-\rho_{\min})\cdot(\rho_{\max}+\rho_{\min})^{-1} \quad (6)$$

$$A=\sin\delta_B\sin i\sin\omega+\cos\delta_B[\cos(\Omega-\alpha_B)\cos\omega$$
$$-\cos i\sin(\Omega-\alpha_B)\sin\omega] \quad (7)$$

$$B=\sin\delta_B\sin i\cos\omega-\cos\delta_B[\cos(\Omega-\alpha_B)\sin\omega$$
$$+\cos i\sin(\Omega-\alpha_B)\cos\omega] \quad (8)$$

$$c=1/2\beta r_p\epsilon\sin^2 i \quad (9)$$

A and B can be thought of as modulation coefficients dependent on the orientation and placement of the satellite orbit (i,ω,Ω) relative to the bulge center. The bulge location is defined by its right ascension, α_B, and its declination, δ_B. The right ascension of the orbit is given by Ω.

It has been shown [3,4] that the changes in semimajor axis a, the quantity (ae), and perigee argument ω, due to air drag on a per-orbit rev basis are:

$$\Delta a=-\delta a^2\int_0^{2\pi}\rho(1+e\cos E)^{3/2}$$
$$\cdot(1-e\cos E)^{-1/2}dE \quad (10)$$

$$\Delta(ae)=-\delta a^2\int_0^{2\pi}\rho(e+\cos E)\ (1+e\cos E)^{1/2}$$
$$\cdot(1-e\cos E)^{-1/2}dE \quad (11)$$

$$\Delta\omega=-\delta(a/e)\int_0^{2\pi}\rho(1+e\cos E)\sin E\,dE \quad (12)$$

δ is a constant parameter that reflects the ballistic coefficient (C_DA_{REF}/m) and a correction factor[1,5] for atmosphere rotation.

$$\delta=(C_DA_{\text{REF}}/m)\ (1-(r_p/V_p)\Lambda\omega_e\cos i)^2 \quad (13)$$

Λ is the ratio of atmosphere angular rotation to the earth's rotation, ω_e, and V_p is the perigee velocity.

Transforming true anomaly into eccentric anomaly in Eq. (4) and expressing Eqs. (4,10-12) in series expansions to the first order in e, the following is obtained with the substitution of Eq. (4) into Eqs. (10-12).

$$\Delta a=-\delta\rho_0a^2\exp[-\beta\,ae-c\cos 2\omega]$$
$$\cdot\int_0^{2\pi}\{1+FA\cos E-eFA+eFA\cos^2E$$
$$+FB\sin E+eFB\sin E\cos E\}$$
$$\cdot\{1+c\cos 2(\omega+E)-2ec\sin 2(\omega+E)\sin E$$
$$+1/4c^2+1/4c^2\cos 4(\omega+E)-ec^2\sin 4(\omega+E)$$
$$\sin E\}\cdot\{1+2e\cos E\}\exp[\beta ae\cos E]dE \quad (14)$$

$$\Delta(ae)=-\delta\rho_0a^2\exp[-\beta ae-c\cos 2\omega]$$
$$\int_0^{2\pi}\{\text{same}\}\cdot\{\text{same}\}\cdot\{\cos E+e+e\cos^2E\}\cdot\exp[\beta\,ae\cos E]dE \quad (15)$$

$$\Delta\omega=-\delta\rho_o(a/e)\exp[-\beta ae-c\cos 2\omega]$$
$$\int_0^{2\pi}\{\text{same}\}\cdot\{\text{same}\}\cdot\{\sin E+e\sin E\cos E\}\cdot\exp[\beta ae\cos E]dE \quad (16)$$

Note that the first two integrand terms in Eqs. (15) and (16) are identical to the first terms in Eqs. (14). Equations (14-16) can be further expanded so that integrand terms are in the form of multiple angles; i.e., cos (nE) which is the integrable representation of the Bessel function of the first kind and imaginary argument $I_n(z)$ where $z=\beta ae$.

$$I_n(z)=\frac{1}{2\pi}\int_0^{2\pi}\cos(nE)\exp[z\cos E]dE \quad (17)$$

The perturbations in orbit parameters can now be obtained over one orbit revolution in terms of Bessel functions. Equations (14-16) integrated yield:

$$\Delta a=-2\pi\delta\rho_0a^2\exp[-\beta ae-c\cos 2\omega]$$
$$\cdot\{I_0+2eI_1+FA[I_1+1/2e(I_0+3I_2)]$$
$$+c\{I_2+2eI_3+1/2FA[I_1+I_3$$
$$+1/2e(I_0+2I_2+5I_4)]\}\cos 2\omega$$
$$-1/2cFB\{I_1-I_3+1/2e(I_0+4I_2-5I_4)\}\sin 2\omega$$
$$+1/4c^2\{I_0+2eI_1+FA[I_1+1/2e(I_0+3I_2)]\}$$
$$+1/4c^2\{I_4-e(I_3-3I_5)+1/2FA[I_3+I_5$$
$$-1/2e(I_2-2I_4-7I_6)]\}\cos 4\omega$$
$$-1/8c^2FB\{I_3-I_5-1/2e(I_2-8I_4+7I_6)\}\sin 4\omega\} \quad (18)$$

$$\Delta(ae)=-2\pi\delta\rho_0a^2\exp[-\beta ae-c\cos 2\omega]$$
$$\cdot\{I_1+1/2e(3I_0+I_2)+1/2FA[I_0+I_2$$
$$+e(3I_1+I_3)]$$
$$+1/2c\{I_1+I_3-1/2e(I_0-6I_2-3I_4)$$
$$+1/2FA[I_0+2I_2+I_4+e(I_1+2I_3$$
$$+I_5)]\}\cos 2\omega$$
$$-1/4cFB\{I_0-I_4+2e(2I_1-I_3-I_5)\}\sin 2\omega$$
$$+1/4c^2\{I_1+1/2e(3I_0+I_2)+1/2FA$$
$$\cdot[I_0+I_2+e(3I_1+I_3)]\}$$
$$+1/8c^2\{I_3+I_5-1/2e(3I_1-6I_4-5I_6)$$
$$+1/2FA[I_2+2I_4+I_6+e(3I_1+5I_3$$
$$+I_5+3I_7)]\}\cos 4\omega$$
$$-1/16c^2FB\{I_2-I_6+e(3I_1-3I_3-I_5+3I_7)\}$$
$$\cdot\sin 4\omega\} \quad (19)$$

$$\Delta\omega = -\pi\delta\rho_o(a/e)\exp[-\beta ae - c\cos 2\omega]$$
$$\cdot\{FB[I_o - I_2 + e(I_1 - I_3)]$$
$$-c[I_1 - I_3 - 1/2e(I_0 - 4I_2 + 3I_4) + 1/2FA\{I_o$$
$$-I_4 - 2e(I_3 - I_5)\}]\sin 2\omega$$
$$-1/2cFB[I_o - 2I_2 + I_4 + e(2I_1 - 4I_3 + 2I_5)]\cos 2\omega\} \quad (20)$$

These equations when compared to oblate atmosphere decay theory,[2] show additional terms involving FA and FB due to bulge effects. As will be shown subsequently, these terms can contribute over 10% to the total decay rates. The change in orbit eccentricity is found from,

$$\Delta e = [\Delta(ae) - e\Delta a] \div [a] \quad (21)$$

The corresponding orbit period decay rate is $\dot{\tau}$.

$$\dot{\tau} = 3/2\ (\tau/a)\,\Delta a(\text{per orbit rev}) \quad (22)$$

Gravitational Perturbations

In the previous equations for determining orbit decay rates, the osculating perigee radius, r_p, and argument, ω, must be estimated with reasonable accuracy since both σ and ρ_0 are directly involved. Usually, a set of osculating orbit elements is assumed known or is available at some perigee passage having an instantaneous perigee argument ω. However, the set is not constant and will be different for another value of ω because of the asymmetries in the earth mass. In fact, as the apse precesses, r_p can vary by ± 5 naut mile (± 9 km) around some mean value $\bar{r}_p$. This variation can easily lead to errors of over 15% in the prediction of decay rates as illustrated in Table 1. Kozai[6] has shown that if the mean orbital elements are known, osculating values can be computed at any time simply by adding the long periodic and short periodic perturbations to the mean values. By reversing the process, mean elements can be obtained by subtracting short and long periodic perturbations from the osculating values.

Therefore, if the osculating perigee values of a,e,i and ω are initially known at t_o, their mean values ($\bar{a}$, $\bar{e}$, $\bar{\omega}$) can be found in the following manner. First, from Kozai,[7] the three parameters $F(i)$ $F'(i)$ and P can be defined.

$$F(i) = (8 - 28\sin^2 i + 21\sin^4 i)/(4 - 5\sin^2 i) \quad (23)$$

$$F'(i) = (64 - 432\sin^2 i + 792\sin^4 i - 429\sin^6 i)$$
$$/(4 - 5\sin^2 i) \quad (24)$$

$$P = 3/4(1/p)\{A_3/A_2 - 5/4(A_5/A_2)\ (1/p)^2 F(i)$$
$$+ 35/128(A_7/A_2)\ (1/p)^4 F'(i)$$
$$(p = a[1 - e^2]) \quad (25)$$

Table 1 Effect of perigee perturbations on decay rates[a]

Perigee arg. (deg)		Period decay rate, $\dot{\tau}$ (sec/rev)	
$\bar{\omega}$	ω	Unperturbed ($\bar{r}_p$)	Perturbed (r_p)
0	3.614	0.06205	0.05472
90	90.000	0.05971	0.06450
180	176.386	0.08607	0.07651
270	270.000	0.06235	0.05116

[a] $\bar{a} = 3663.58$ nm (6784.95 km), $\bar{e} = 0.2$, $i = 90°$, $\Omega = 33.3°$, 9/22/75: 0 hr.

Next, the mean argument of perigee[6] is estimated.

$$\bar{\omega} = \omega - A_2/p^2[(1/(3e) + 4e/3 + 13/8)\sin^2 i$$
$$-1/2 - 2e/3]\sin 2\omega - (1/e)P\sin i\cos\omega \quad (26)$$

Knowing $\bar{\omega}$, the mean orbit eccentricity[6] is;

$$\bar{e} = e - 1/2(A_2/p^2)[1/e(2/3 - \sin^2 i)$$
$$\{(1+e)^3 - (1-e^2)^{3/2}\}$$
$$+ (5/3 + 3e + e^2)\sin^2 i\cos 2\omega]$$
$$-(1-e^2)^{3/2}\} + (5/3 + 3e + e^2)\sin^2 i\cos 2\omega]$$
$$-(1-e^2)P\sin i\sin\bar{\omega} \quad (27)$$

and the mean semimajor axis[6] is found by:

$$\bar{a} = a - (A_2/p)\ (1-\bar{e}^2)^{-2}[(2/3 - \sin^2 i)\{(1+\bar{e})^3$$
$$-(1-\bar{e}^2)^{3/2}\} + (1+\bar{e})^3\sin^2 i\cos 2\omega] \quad (28)$$

In Eqs. (25-28), A_2, A_3, A_5, and A_7 are the Kozai[6] defined harmonic coefficients of the potential function. The equations reflect the perturbations in a (7,0) geopotential field; i.e., the potential in expanded spherical harmonics up to the 7th cosine harmonic coefficient,[8] C_{lm} ($l = 0$ to 7, $m = 0$), and without any sine harmonic coefficients (S_{lm}). After some elapsed revs Δn, $\bar{\omega}$ will precess at a secular rate $\dot{\bar{\omega}} + \Delta\omega$; and $\bar{a}$ and $\bar{e}$ will decrease at their decay rates to new mean values. The corresponding changes in inclination i and right ascension Ω due to drag decay can be determined from Refs. 5 and 9. Osculating perigee conditions at $t_0 + \Delta n$ are calculated easily by replacing $\sin 2\omega$, $\cos\omega$, e and a in Eq. (26) with $\sin 2\bar{\omega}$, $\cos\bar{\omega}$, $\bar{e}$, $\bar{a}$ and solving for the value of ω. Equations (27) and (28) can then be used to solve for the values of a and e. The perigee radius at the time of perigee passage ($t_0 + \Delta n$) is $r_p = a(1-e)$. The inaccuracy of r_p as determined in this described manner without iteration is less than 0.2 naut mile (0.37 km). It is not necessary to use $\bar{i}$ or $\bar{\Omega}$ since their variations are relatively small and consequently have negligible impact on the magnitude of the perturbations of $\bar{a}$, $\bar{e}$ and $\bar{\omega}$.

It is important to note that the values of a and (ae) used in Eqs. (18-20) must actually be replaced by the geometric orbit shape a_{GEOM} and $(ae)_{\text{GEOM}}$ values defined by the osculating perigee and apogee radii at their respective passages. Therefore, the geometric factor $(ae)_{\text{GEOM}}$ is found by adding the long-term perturbations to the mean perigee values; this is equivalent to the following noting that $a_{\text{GEOM}} = \bar{a}$.

$$(ae)_{\text{GEOM}} \equiv \bar{a}e' \quad (29)$$

where

$$e' = \bar{e} + (1-\bar{e}^2)P\sin i\sin\bar{\omega} \quad (30)$$

As a matter of interest, the corresponding osculating apogee radius is $r_a = r_p + 2\bar{a}e'$.

Scale Height Selection

These decay rate equations require the use of a constant scale height, H. It is known that density scale height increases with altitude and this variation can give rise to errors in decay rate predictions. This problem was addressed by King-Hele and Scott,[9] and it was concluded that the constant H theory could be used if H is evaluated at a distance $3/4H$ above perigee. The "$3/4H$" theory, however, does not include the additional combined effects of the oblate earth figure and bulge. For example, H actually has an approximate sinusoidal variation on the constant altitude surface (Fig. 1) similar to

the density variations. This sinusoidal H variation can cause a 60% increase or decrease in the H increment evaluated between r_p and $r_p+3/4H$. In addition, increasing altitude, due to the earth's flattening over polar regions can increase this discrepancy. However, it was noted that density could be predicted within a few percent in the high-drag region by using the local H value on the constant altitude surface. Therefore, it is assumed that a more suitable H could be evaluated using the local H value at an orbit true anomaly which represented the average flight density (the average density point being 50% of the perigee density value). This action, in a sense, is tantamount to that of the "3/4H" theory.[9] For example, an orbit with a large eccentricity will have its high-drag regime in the vicinity of perigee, and therefore, H is evaluated close to perigee. As the eccentricity approaches small values, the H value approaches the sinusoidal average. Now, the average fractional change $F_r(\rho/\rho_P)_{\text{BULGE}}$ from the perigee density value on the constant altitude surface is obtained from Eq. (4) averaged for values of $+\theta$ and $-\theta$.

$$F_r(\rho/\rho_P)_{\text{BULGE}} = [1+FA\cos\theta]\cdot[1+FA]^{-1}-1 \quad (31)$$

For small eccentricities, the fractional change $F_r(\rho/\rho_p)_{\text{ALT}}$ from the perigee density value due to orbit altitude gain is approximated by Eq. (32) with $z=\beta ae$.

$$F_r(\rho/\rho_P)_{\text{ALT}} = -z(1-\cos\theta)+1/2\ z^2(1-\cos\theta)^2 \quad (32)$$

For a density decrease of 50% (equivalent to a fractional change of -0.5), the following is written.

$$F_r(\rho/\rho_P)_{\text{BULGE}}+F_r(\rho/\rho_P)_{\text{ALT}} = -0.5 \quad (33)$$

From Eq. (34), the average true anomaly θ_{AVG} can be solved for

$$\cos\theta_{\text{AVG}} = 1/z^2[Z_1+\{-Z_1^2-2z^2Z_2\}^{1/2}] \quad (34)$$

where

$$Z_1 = z(z-1)-FA\cdot(1+FA)^{-1} \quad (35)$$

and

$$Z_2 = (1+FA)^{-1}-z(1-1/2z)-0.5 \quad (36)$$

If the quantity in the brackets { } of Eq. (34) is negative, then $\theta_{\text{AVG}}=90°$. Generally this quantity becomes negative for small eccentricities when A is negative and large; i.e., when perigee is approaching 180° separation from the bulge. Equation (34) points out that a small value of eccentricity ($e\sim 0.01$) will be a threshold value in many cases for taking $\theta_{\text{AVG}}=90°$ rather than $e=0$.

As was done with density, the scale height H can be represented as a cosine function on the constant altitude surface.

$$H = H_0+S[A\cos\theta+B\sin\theta] \quad (37)$$

where H_0 is average scale height, $H_0=1/2(H_{\text{MAX}}+H_{\text{MIN}})$ and $S=(H_{\text{MAX}}-H_{\text{MIN}})(H_{\text{MAX}}+H_{\text{MIN}})^{-1}$. Actually the scale heights associated with the double valued θ_{AVG} may not be balanced; i.e., their differences between the perigee value may not be equal. After evaluating Eq. (37) for $+\theta_{\text{AVG}}$ and $-\theta_{\text{AVG}}$, an average height, H_{AVG} can be expressed by

$$H_{\text{AVG}} = H_0+SA\cos\theta_{\text{AVG}} \quad (38)$$

Table 2 indicates that the "3/4H" theory, although adequate when perigee is located opposite the atmospheric bulge, can lead to errors of 5% when perigee is close to the bulge center. Table 2 shows a comparison of decay rates using the "3/4H" theory and the derived expression (38) with numerically integrated data for reference. In Table 2 and succeeding data, the use of Eq. (38) appears to be quite adequate considering atmosphere model uncertainties for decay rate prediction.

Table 2 Effect of scale height selection on decay rates[a]

	Period Decay Rate, $\dot{\tau}\sim$ sec/rev		
$\bar{\omega}$	"3/4H" theory[9]	H from Eq. (36)	Orbit integration
0° (Perigee opposite bulge)	0.05540	0.05423	0.05472
180° (Perigee in bulge)	0.08010	0.07639	0.07652

[a] $\bar{a}=3663.58$ nm(6784.95 km), $\bar{e}=0.02$, $i=90°$, $\Omega=33.3°$, 9/22/75; 0 hr.

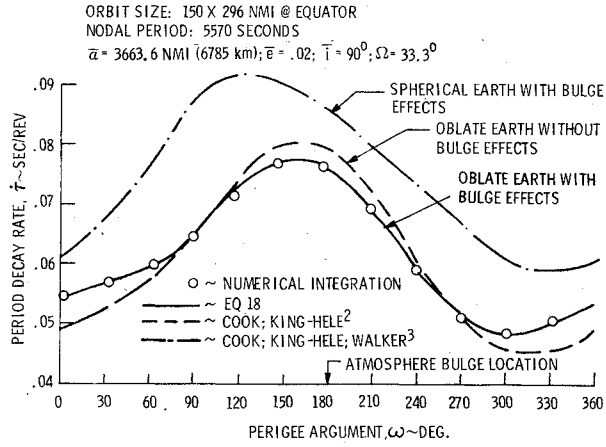

Fig. 2 Orbit period decay rate comparison (case 1).

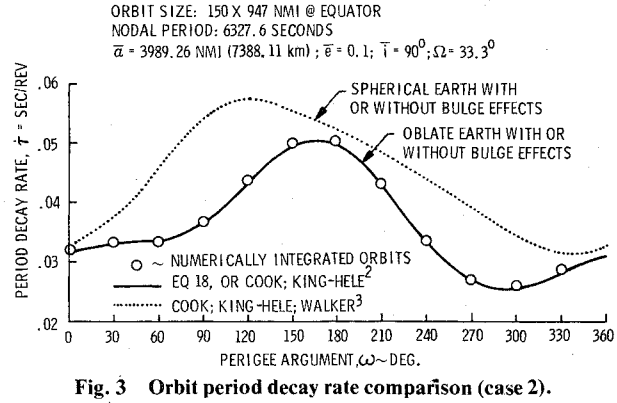

Fig. 3 Orbit period decay rate comparison (case 2).

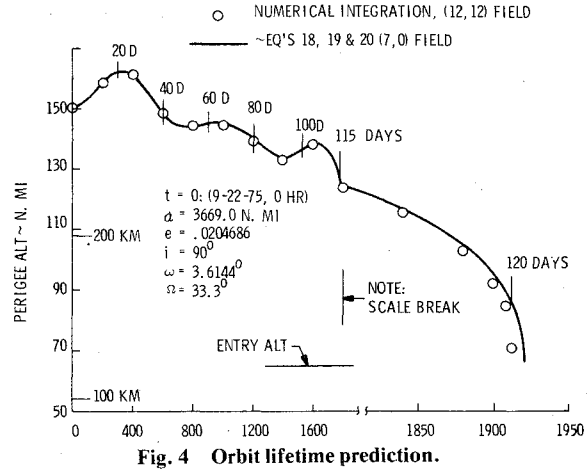

Fig. 4 Orbit lifetime prediction.

Possibly, additional rigorous treatment of scale height increase with altitude and earth's flattening, together with the sinusoidal H variation may yield still more accurate results.

Numerical Results

The equations above were evaluated using a modified Jacchia 1967 atmosphere[10] for several sample cases. The average density, ρ_0, was adjusted to ρ_0' to insure an accurate cosine density fit in the perigee region where the greatest perturbation effects are experienced. This adjustment is a result of the sinusoidal density variation assumption [Eq. (3)] which is not an exact representation of the Jacchia atmosphere model, and generally is on the order of 1% or less

$$\rho_0' = \rho_P - \rho_0 FA \tag{39}$$

where ρ_P is perigee density.

Atmosphere conditions reflected in the following figures consisted of a mean solar flux value at the 10.7 cm wavelength of $FL = 150 \cdot 10^{-22}$ watts/m^2/cps and a geomagnetic activity index $a_p = 20$ ($2 \cdot 10^{-5}$ gauss). Figure 2 presents a comparison of instantaneous decay rates of the effective or average nodal period with a (5,0) geopotential gravity field. The date selected for density computations is 0 HR, September 22, 1975; which places the sun at the autumnal equinox position. The mean orbital elements selected result in osculating perigee and apogee altitudes of 150.0 nmi and 296.4 naut mile respectively (277×548.93 km) when $\omega = 0$; and with a mean nodal period of 5570 sec. A right ascension of 33.3° places the orbit plane nearly at the center of the bulge. An inclination of 90° was taken since the effects of the oblate earth figure are most pronounced in this case. In the numerical examples, the ballistic coefficient was taken as a constant, $C_D A_{REF}/m = 2.0$ ft^2/slug, and atmosphere rotation factor Λ as unity. It can be seen that the available spherical earth theory with bulge effects can result in decay rate errors of 35%; while oblate earth theory without bulge effects can lead to errors of over 10%. Therefore, the inclusion of bulge effects with the oblate earth theory is essential to obtaining a higher inherent accuracy. A comparison of Eqs. (18) and (19) results with numerical integration results shows that accuracies within 2% or less can be obtained. A similar comparison is made in Fig. 3 for an orbit having a mean eccentricity of 0.1 which gives a 150.0×946.9 naut mile (277.8×1753.7 km) at the equator and with a nodal period of 6327.6 sec. This figure indicates that the bulge effects are essentially negligible for an orbit eccentricity of 0.1 or greater. Again it is noted that the oblate earth theory gives the more accurate results. Therefore, for eccentricities greater than 0.1, either the oblate theory[2] can be used or the e^2 terms given in the oblate theory can be added to Eqs. (18) and (19) to achieve the same accuracy.

Figure 4 presents a perigee altitude history prediction for an orbit having an approximate 120-day lifetime. Entry, as predicted using Eqs. (18-20), occurs less than 10 revs later than that computed through numerical integration. If the prediction process were updated at 1800 revs, then the predicted entry is within 1 rev of the numerically integrated value of 1912 revs. Computational time for integrating an orbit in a (12, 12) geopotential field for 1900 revolutions can require up to 6 hr depending on the specific digital program. The corresponding computation time using the prediction equations is less than four minutes by comparison.

Conclusions

Equations are presented that allow the prediction of orbit drag perturbations in terms of decay rates over an oblate earth with a diurnal atmosphere bulge. The intrinsic accuracy of the perturbation equations is within 2% when used with a modified Jacchia 1967 atmosphere model. Therefore, in operational flight, additional perturbation errors will be a result only of atmosphere model and ballistic coefficient uncertainties. The perturbation equations are useful either as a design study tool for rapid decay rate and lifetime prediction or as an expedient means for inflight monitoring and control of operational satellites. In its inverse form, the theoretical expressions can also be used to solve for the effective ballistic coefficient when given an observed decay rate of an orbiting satellite. Finally, the developed expressions can be utilized to isolate drag effects for the determination of various earth dynamical constants or atmosphere related parameters.

References

[1] Cook, G. E., "Effect of an Oblate, Rotating Atmosphere on the Orientation of a Satellite Orbit," RAE TN 6. W.550, June 1960, Royal Aircraft Establishment, Farnborough, England.

[2] Cook, G. E., King-Hele, D.G. and Walker, D.M., "The Contraction of Satellite Orbits Under the Influence of Air Drag—Part II, With Oblate Atmosphere," *1961 Proceedings of the Royal Society*, Vol. 264 pp. 88-121.

[3] Cook, G. E. and King-Hele, D.G., "The Contraction of Satellite Orbits Under the Influence of Air Drag—Part V, With Day-to-Night Variation in Air Density," *Philosophical Transactions of the Royal Society*, Vol. 259, 1965, pp. 33-67.

[4] Cook, G. E. and King-Hele, D.G., "The Contraction of Satellite Orbits Under the Influence of Air Drag. Part VI: Near-Circular Orbits with Day-to-Night Variation in Air Density," TR 67092, April 1967, Royal Aircraft Establishment, Farnborough, England.

[5] King-Hele, D.G., and Walker, D.M., "The Change in Satellite Orbital Inclination Caused by a Rotating Atmosphere With Day-to-Night Density Variation," *Celestial Mechanics*, Vol. 5, Jan. 1972, pp. 41-54.

[6] Kozai, Y., "The Motion of a Close Earth Satellite," *Astronautical Journal*, Vol. 64, Nov. 1959, pp. 367-377.

[7] Kozai, Y., "The Gravitational Field of the Earth Derived from Motions of Three Satellites," *Astronautical Journal*, Vol. 66, Feb. 1961, pp. 8-10.

[8] Kaula, W., *Theory of Satellite Geodesy*, Blaisdell Pub. Co., Waltham, Mass., 1966.

[9] King-Hele, D.G. and Scott, D.W., "The Effect of Atmospheric Rotation on a Satellite Orbit, When Scale Height, Varies with Height," *Planet Space Science*, Vol. 17, 1969, pp. 217-232.

[10] *Models of Earth's Atmosphere*, SP-8021, Feb. 1969, NASA; available from the Superintendent of Documents, U.S. Gov't Printing Office, Washington, D.C.